

## FIBER BUCKLING IN THREE-DIMENSIONAL PERIODIC-ARRAY COMPOSITES

IRADJ G. TADJBAKHSH

Department of Civil Engineering, Rensselaer Polytechnic Institute, Troy,  
NY 12180-3590, U.S.A.

and

Y. M. WANG

Department of Mechanical Engineering, Rensselaer Polytechnic Institute, Troy,  
NY 12180-3590, U.S.A.

(Received 4 November 1991; in revised form 28 April 1992)

**Abstract**—The in-plane microbuckling of a fully bonded cross-ply laminate composite is considered. The problem is formulated by treating the composites as a single phase inhomogeneous continuum. The fiber and the matrix are accounted for by spatial variation of the moduli of the two phases. The variation of material properties is expressed by a Fourier series expansion in the coordinate directions. Similarly the buckled mode shapes are thought of as three-dimensional Fourier series that satisfy the governing differential equations. These equations are obtained by superposition of small displacements on the finite pre-buckled elastic state.

Our results corroborate the results of Lagoudas *et al.* (1991, *J. Appl. Mech.* **58**, 473–479) which deals with a two-dimensional plane strain situation. In the 3-D case, the effect of ply layup on buckling strength under uniaxial and biaxial compression is determined. The solutions for the critical condition determined by different modes of buckling and certain physical parameters under biaxial compression are also studied.

### INTRODUCTION

Due to their high strength to weight ratio, composites are being used more frequently in lightweight structures, such as space stations, aircraft, submarines, etc. A large amount of research has been performed to construct theories of the behavior of composites. However, an area where the traditional approach has been found to be inadequate is the compressive strength of composite structures, where the compressive failure might occur as both long and short wavelength buckling. A well known feature of the microstructural compression failure is the occurrence of microbuckling and subsequently sudden reduction in the effective compressive strength of the composite. It is widely believed that the fiber buckling plays an important role in the failure phenomenon.

Rosen (1956) considered the stability of a two-dimensional array of layers of fibers bonded to an elastic matrix. An important result that follows from this analysis is that for low fiber volume fraction the extensional buckling mode is the dominant mode of buckling, while for high fiber volume fractions (> 20%) the shear buckling mode is predicted. Chung and Testa (1969) modeled the fibers as beams in an elastic foundation. Similar buckling modes and failure loads to those in Rosen's model are indicated in their analytical and experimental results. Recently, Swanson (1990) considered a 3-D model that includes the effect of resistance of the adjacent plies on the buckling strength of laminas with axial fibers. He indicated that the apparent strength of the axial plies depends on the total laminate layup and that the adjacent plies provide additional shear resistance to fiber microbuckling. Lagoudas *et al.* (1991) developed a 2-D microbuckling model that treated the composite as a single phase and as an inhomogeneous elastic solid. The influence of imperfections is modeled as fiber waviness with a free wavelength parameter. Their results show that compressive strength is substantially lower than predicted by Rosen's analysis. This new approach to microbuckling is also the basis of this paper. It is known that there are situations when in-plane microbuckling requires three-dimensional modeling such as the effect of adjacent layers or various patterns in the periodic arrangement of the fibers. In this study, a three-dimensional structure, i.e. composite plate composed of a number of

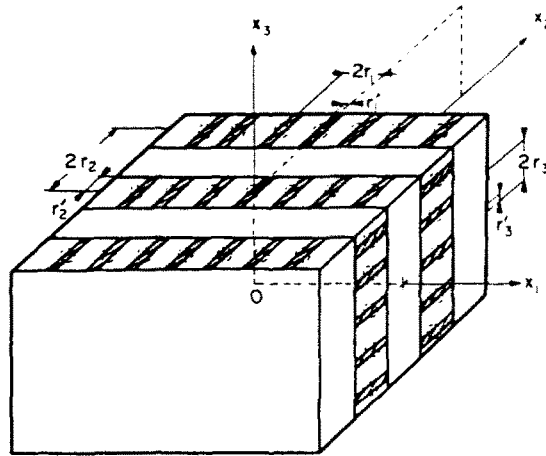


Fig. 1(a). Configuration of the structure.

thin laminae, is considered. An element cut from this kind of structure is shown in Fig. 1(a). As seen from this figure, even if the dimension in one of the three directions is finite, in the  $X_2$  direction say, at the micro-structural scale, local buckling takes place at distances far from the boundary. Therefore, for compressive strength primarily the axial Young's modulus needs to be represented as a variable quantity. The Fourier series with a wavelength equal to the average spacing between fibers is used to take into account the periodicity of the microstructure. In this model a fiber is replaced with a rectangular strip of the same width as the ply and same area as the fiber. The structure consists of bonded laminae with 0 and 90° fiber orientations. The occurrence of microbuckling in the  $X_2$  direction is prevented

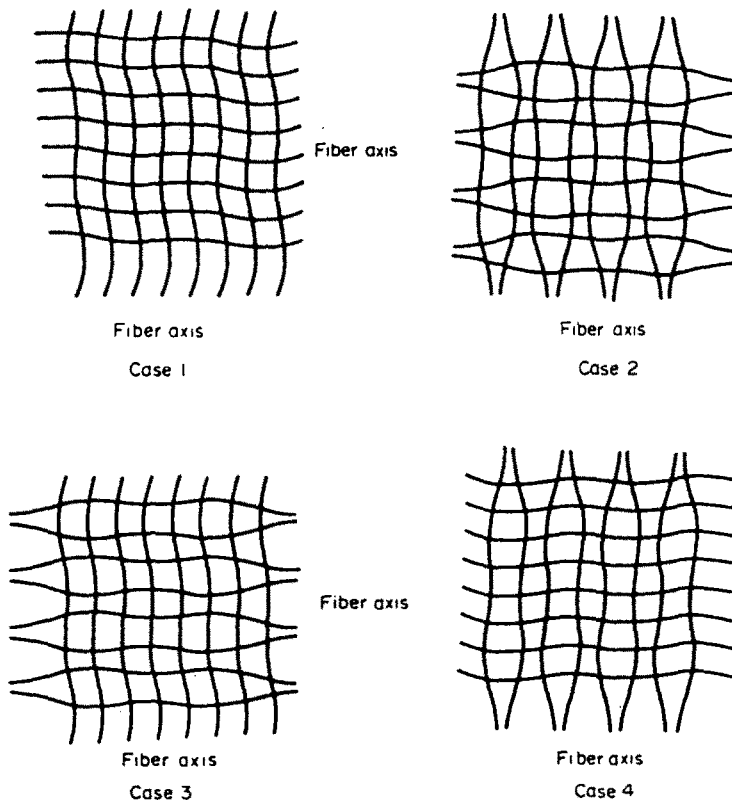


Fig. 1(b). Modes of buckling for cases 1-4 given in Table 1 [front view projection of Fig. 1(a)].

by the adjacent plies. The weak planes are the planes of the laminas to which the buckling modes of fibers are confined. It is mentioned here that the phenomenon of composite delamination is not considered in this paper because it requires the measurement of an interfacial bonding parameter (interface strength) and in some cases [e.g. Steif (1988)] the extent of initial debonding, which is not the topic of interest in the present analysis.

Results of the present analysis show that under certain conditions critical strain of the simplest possible approximation reduces to Rosen's classical results (1956) for compressive buckling strain of fibrous composites in the shear buckling mode. Moreover, it shows that in the absence of cross plies the critical strain depends on the assumed fiber imperfections. The minimum value of the compressive strength occurs in the limit of vanishingly small wavelength of imperfections. It is also observed that the resistance to fiber buckling of the composites can be improved by increasing the shear modulus of the matrix. Our results also show that under uniaxial compression additional resistance to fiber buckling is provided by adjacent plies as the thickness of these plies increases which was also found by Swanson (1990). However, it is observed that for prescribed nonzero strain in one direction, the buckling strain in the other direction will increase within an interval and thereafter decreases with the thickness of these laminas with transverse fibers.

BASIC FORMULAE

We consider a three-dimensional structure consisting of laminas with 0 and 90° fiber orientations with respect to the vertical as shown in Fig. 1(a). The Cartesian coordinates of a material point of the continuum are represented by  $\mathbf{X}$ ,  $\mathbf{X} = (X_1, X_2, X_3)^T$ . In the absence of body forces the equation of equilibrium is (Malvern, 1969),

$$\mathbf{V} \cdot [\mathbf{T} \cdot \mathbf{V}\mathbf{x}] = 0, \tag{1}$$

where  $\mathbf{V}$  is the gradient operator in the Cartesian coordinate frame  $\mathbf{X}$ ;  $\mathbf{x}$  is the position vector after deformation;  $\mathbf{T}$  is the second order Piola Kirchhoff stress tensor. The six components of the stress tensor  $\mathbf{T}$  are denoted by  $\sigma$  which is related to the Green-Lagrange strain  $\epsilon$  through an orthotropic linear elastic Hooke's law that defines the material behavior (Appendix A).

For a periodic matrix structure shown in Fig. 1(a), the variation of Young's moduli  $E_{11}$  and  $E_{33}$  can be expressed by the following Fourier series (Appendix B):

$$E_{11}(X_2, X_3) = E_{11}^v(r_2'/r_2) + E_{11}^h(X_3)(1 - r_2'/r_2) + [E_{11}^v - E_{11}^h(X_3)] \sum_{n=1}^{\infty} \alpha_n^{(2)} \cos \frac{n\pi X_2}{r_2}, \tag{2a}$$

$$E_{33}(X_1, X_2) = E_{33}^v(X_1)(r_2'/r_2) + E_{33}^h(1 - r_2'/r_2) + [E_{33}^v(X_1) - E_{33}^h] \sum_{n=1}^{\infty} \alpha_n^{(2)} \cos \frac{n\pi X_2}{r_2}, \tag{2b}$$

where the superscripts v and h refer to the laminas in which the fibers are oriented in vertical ( $X_3$ ) and horizontal ( $X_1$ ) directions respectively;  $E_{11}^v$  and  $E_{33}^h$  are the effective Young's moduli of the laminas with vertical fibers and of horizontal fibers and are assumed constant. Also  $E_{11}^h(X_3)$  and  $E_{33}^v(X_1)$  are the axial Young's moduli of the laminas with the horizontal and vertical fiber directions and can themselves be represented as Fourier series in the  $X_3$  and  $X_1$  directions respectively:

$$\begin{aligned} E_{11}^h(X_3) &= [E_t(r_3'/r_3) + E_m(1 - r_3'/r_3)] + (E_t - E_m) \sum_{n=1}^{\infty} \alpha_n^{(3)} \cos \frac{n\pi X_3}{r_3} \\ &\equiv \frac{1}{2} D_0^* + \sum_{n=1}^{\infty} D_n^* \cos \frac{n\pi X_3}{r_3}, \end{aligned} \tag{3a}$$

$$\begin{aligned}
 E_{33}^*(X_1) &= [E_f(r'_1/r_1) + E_m(1 - r'_1/r_1)] + (E_f - E_m) \sum_{n=1}^{\infty} x_n^{(1)} \cos \frac{n\pi X_1}{r_1} \\
 &\equiv \frac{1}{2} C_0^* + \sum_{n=1}^{\infty} C_n^* \cos \frac{n\pi X_1}{r_1}.
 \end{aligned} \tag{3b}$$

Here  $x_n^{(i)} = (2/n\pi) \sin(n\pi r'_i/r_i)$ ,  $i = 1, 2, 3$ ;  $E_f$  and  $E_m$  are the Young's moduli of fiber and matrix respectively. As shown in Fig. 1(a), we note that the spacing ratios  $r'_1/r_1$  and  $r'_3/r_3$  denote the fiber volume fractions  $C_f^*$  and  $C_m^*$  of the layers with vertical and horizontal fibers, respectively. Also,  $2r'_2$  and  $2r_2$  are the thickness of the laminae with vertical fibers and the distance between the midpoint of two plies with vertical fibers separated by one ply with horizontal fibers, respectively. Thus, the thickness of the layers with horizontal fibers is given as  $(2r_2 - 2r'_2)$ . The ratio  $r'_2/r_2$  is then the normalized thickness of the lamina with vertical fibers that is present in one period ( $2r_2$ ) in the  $X_2$  direction.

Prior to buckling, the body is assumed to be in the state of plane strain with  $u_1 = u_1(X_1)$  and  $u_3 = u_3(X_3)$  being the only nonzero components of displacements.

Equilibrium requires that  $u_1 = -a_1 X_1$  and  $u_3 = -a_3 X_3$  where  $a_1$  and  $a_3$  are constants assumed to be positive to signify compression. Superimposing the incremental displacement  $U$ ,  $U = (U_1, U_2, U_3)$ , upon the pre-buckling displacement field, we have

$$u_1 = -a_1 X_1 + \varepsilon U_1(X_1, X_2, X_3), \tag{4a}$$

$$u_2 = \varepsilon U_2(X_1, X_2, X_3), \tag{4b}$$

$$u_3 = -a_3 X_3 + \varepsilon U_3(X_1, X_2, X_3), \tag{4c}$$

where  $\varepsilon$  is a small parameter. The Green-Lagrange strain components are determined to be

$$\begin{aligned}
 \varepsilon_{11} &= (-a_1 + \frac{1}{2}a_1^2) + \varepsilon(1 - a_1)U_{1,1} + O(\varepsilon^2) \\
 &\equiv -b + \varepsilon(1 - 2b)^{1/2}U_{1,1} + O(\varepsilon^2), \quad ( )_{,i} = \frac{\partial}{\partial X_i}, \quad i = 1, 2, 3,
 \end{aligned} \tag{5a}$$

$$\varepsilon_{22} = \varepsilon U_{2,2} + O(\varepsilon^2), \tag{5b}$$

$$\varepsilon_{33} = (-a_3 + \frac{1}{2}a_3^2) + \varepsilon(1 - a_3)U_{3,3} + O(\varepsilon^2) \equiv -d + \varepsilon(1 - 2d)^{1/2}U_{3,3} + O(\varepsilon^2), \tag{5c}$$

$$2\varepsilon_{23} = \varepsilon[U_{2,3} + (1 - 2d)^{1/2}U_{3,2}] + O(\varepsilon^2), \tag{5d}$$

$$2\varepsilon_{13} = \varepsilon[(1 - 2b)^{1/2}U_{1,3} + (1 - 2d)^{1/2}U_{3,1}] + O(\varepsilon^2), \tag{5e}$$

$$2\varepsilon_{12} = \varepsilon[(1 - 2b)^{1/2}U_{1,2} + U_{2,1}] + O(\varepsilon^2). \tag{5f}$$

Also the position of a material point is given by

$$\mathbf{x} = \mathbf{u} + \mathbf{X} \equiv \mathbf{A}\mathbf{x} + \varepsilon\mathbf{U}, \tag{6}$$

where

$$\mathbf{A} = \text{diag}[(1 - 2b)^{1/2}, 1, (1 - 2d)^{1/2}]$$

and  $a_1 = 1 - (1 - 2b)^{1/2}$  and  $a_3 = 1 - (1 - 2d)^{1/2}$ . For  $0 \leq (b, d) \leq \frac{1}{2}$  we have  $0 \leq (a_1, a_3) \leq 1$ . We substitute eqns (2)–(6) with the components of the stiffness matrix  $\mathbf{L}$ , defined by Appendix A into eqn (1) and note that the zeroth order equations are identically satisfied while the first order equations yield

$$\mathcal{L}'\mathbf{U} = 0, \tag{7}$$

where  $\mathcal{L}'$  is a  $3 \times 3$  symmetric matrix operator that is defined in Appendix C. Since the

occurrence of microbuckling in the  $X_2$ -direction is prevented by the adjacent plies, we assume  $U_2 = 0$ . The weak planes are the planes of the laminae to which the buckling modes of the fibers are confined. Based on the above assumption eqns (7), in the  $X_1$  and  $X_3$  directions, become

$$\mathcal{L}_{11}U_1 + \mathcal{L}_{13}U_3 = 0, \tag{8a}$$

$$\mathcal{L}_{13}U_1 + \mathcal{L}_{33}U_3 = 0, \tag{8b}$$

while in the  $X_2$  direction we have

$$\frac{\partial}{\partial X_2} \left( K_1 \frac{\partial U_1}{\partial X_1} + K_3 \frac{\partial U_3}{\partial X_3} \right) = 0, \tag{9}$$

where

$$K_1 = (1 - 2b)^{-1/2} (G_{12} + E_{12}),$$

$$K_3 = (1 - 2d)^{-1/2} (G_{23} + E_{23}).$$

The nonzero incremental displacements are assumed periodic in the  $X_2$  direction as:

$$U_1 = \sum_{j=0}^{\infty} A_j \cos \frac{j\pi X_2}{r_2}, \tag{10a}$$

$$U_3 = \sum_{j=0}^{\infty} B_j \cos \frac{j\pi X_2}{r_2}, \tag{10b}$$

with the coefficients  $A_j$  and  $B_j$  periodic functions of  $X_1$  and  $X_3$  which temporarily are not explicitly stated. We noted that (9) together with (10) imply existence of potential functions  $V_i(X_1, X_3)$ ,  $i = 1, 2, 3, \dots$ , such that

$$A_i = K_3 \frac{\partial V_i}{\partial X_3}, \quad B_i = -K_1 \frac{\partial V_i}{\partial X_1}, \quad i = 1, 2, 3, \dots, \tag{11}$$

where  $A_0$  and  $B_0$  remain unrestricted. Substitution of (10) and (11) into (8) leads to

$$\mathcal{L}_{11}U_1 + \mathcal{L}_{13}U_3 \equiv \sum_{j=0}^{\infty} C_j \cos \frac{j\pi X_2}{r_2} = 0, \tag{12a}$$

$$\mathcal{L}_{13}U_1 + \mathcal{L}_{33}U_3 \equiv \sum_{j=0}^{\infty} D_j \cos \frac{j\pi X_2}{r_2} = 0, \tag{12b}$$

where the coefficients  $C$  and  $D$  are defined differently for  $j = 0$  and  $j \geq 1$ . We have for  $j = 0$ :

$$C_0 \equiv \beta_{11}(X_3)A_{0,11} + \beta_{12}(X_1)A_{0,33} + b_{13}B_{0,13} + \frac{1}{2}K_3\beta_{13}(X_3) \sum_{n=1}^{\infty} \alpha_n^{(2)} V_{n,311} + \frac{1}{2}K_3\beta_{14}(X_1) \sum_{n=1}^{\infty} \alpha_n^{(2)} V_{n,333} = 0, \tag{12a_1}$$

$$D_0 \equiv \beta_{31}(X_3)B_{0,11} + \beta_{32}(X_1)B_{0,33} + b_{13}A_{0,13} - \frac{1}{2}K_1\beta_{33}(X_3) \sum_{n=1}^{\infty} \alpha_n^{(2)} V_{n,111} - \frac{1}{2}K_1\beta_{34}(X_1) \sum_{n=1}^{\infty} \alpha_n^{(2)} V_{n,133} = 0, \tag{12b_1}$$

and for  $j \geq 1$ :

$$\begin{aligned}
 C_j \equiv & \beta_{13}(X_3)\alpha_j^{(2)}A_{0,11} + \beta_{14}(X_1)\alpha_j^{(2)}A_{0,33} + (K_3\beta_{11}(X_3) \\
 & - K_1b_{13})V_{j,311} + K_3\beta_{12}(X_1)V_{j,333} + \frac{1}{2}K_3 \sum_{n=1}^{\infty} \{[\alpha_{j-n}^{(2)}[u(j-n-1) \\
 & + u(n-j-1)](1-\delta_{jn}) + \alpha_{(j+n)}^{(2)}][\beta_{13}(X_3)V_{n,311} + \beta_{14}(X_1)V_{n,333}]\} \\
 & - K_3b_{12}\left(\frac{i\pi}{r_2}\right)^2 V_{j,3} = 0, \quad j = 1, 2, 3, \dots,
 \end{aligned} \tag{12a_2}$$

$$\begin{aligned}
 D_j \equiv & \beta_{33}(X_3)\alpha_j^{(2)}B_{0,11} + \beta_{34}(X_1)\alpha_j^{(2)}B_{0,33} - (K_1\beta_{32}(X_1) \\
 & - K_3b_{13})V_{j,133} - K_1\beta_{31}(X_3)V_{j,111} - \frac{1}{2}K_1 \sum_{n=1}^{\infty} \{[\alpha_{j-n}^{(2)}[u(j-n-1) \\
 & + u(n-j-1)](1-\delta_{jn}) + \alpha_{(j+n)}^{(2)}][\beta_{33}(X_3)V_{n,111} + \beta_{34}(X_1)V_{n,133}]\} \\
 & + K_1b_{32}\left(\frac{i\pi}{r_2}\right)^2 V_{j,1} = 0, \quad j = 1, 2, 3, \dots
 \end{aligned} \tag{12b_2}$$

Here the subscript  $|j-n|$  has the usual properties that  $|j-n| = j-n$  for  $j \geq n$  and  $|j-n| = n-j$  for  $j < n$ ; the function  $u(j-n)$  is defined as  $u(j-n) = 1$  for  $j \geq n$  and  $u(j-n) = 0$  for  $j < n$ ; and  $\delta_{mn}$  is the Dirac delta symbol. The coefficients  $\beta_{11}, \beta_{12}, \dots$ , and  $b_{12}, b_{13}$  and  $b_{32}$  are given in Appendix D. It is noted that the coefficient functions  $C_j$  and  $D_j$  must identically vanish. Vanishing of Cs and Ds provides two infinite sets of equations. Each member of these sets is to be further expanded as a Fourier series in the remaining two directions, i.e.  $X_1$  and  $X_3$ . Observing (12) we find that these equations admit more symmetries in solutions in the  $X_1, X_3$  plane than the shear and the extensional modes observed in the two-dimensional plane strain case. These symmetries can be expressed in terms of oddness or evenness of  $A_0, B_0$  and  $V_n, n = 1, 2, 3, \dots$ , as functions of  $X_1$  and  $X_3$  and can be given in tabular form. There are four possible symmetries as given in Table 1 and illustrated in Fig. 1(b).

Correspondingly, the functions  $A_0, B_0$  and  $V_n$  can be expressed in Fourier sine or cosine series that reflect those symmetries. It is noted that the mode shapes assumed in cases 1 and 2 are analogous to the modes of buckling introduced by Lagoudas *et al.* (1991) for compressive strain of fibrous composites in the shear and extensional buckling modes respectively. The buckling modes of  $A_0, B_0$  and  $V_n$  for each case are assumed to be:

$$A_0 = \sum_{i=0}^{\infty} \sum_{k=0}^{\infty} A_{ik} \Psi_{ik}^m, \tag{13a}$$

$$B_0 = \sum_{i=0}^{\infty} \sum_{k=0}^{\infty} B_{ik} \varphi_{ik}^m, \tag{13b}$$

$$V_n = \sum_{i=0}^{\infty} \sum_{k=0}^{\infty} V_{ik}^n \phi_{ik}^m, \tag{13c}$$

where the superscript  $m, m = 1, 2, 3, 4$ , is the number of the corresponding case;  $A_{ik}, B_{ik}$  and  $V_{ik}^n$  and correspondingly  $\Psi_{ik}^m, \varphi_{ik}^m$  and  $\phi_{ik}^m$  are the amplitudes and the mode shapes of  $A_0, B_0$  and  $V_n$ , respectively, for the cases 1-4 given by Table 1. Here  $i$  and  $k$ ,

Table 1

	Case 1		Case 2		Case 3		Case 4	
	$X_1$	$X_3$	$X_1$	$X_3$	$X_1$	$X_3$	$X_1$	$X_3$
$A_0$	even	odd	odd	even	even	even	odd	odd
$B_0$	odd	even	even	odd	odd	odd	even	even
$V_n$	even	even	odd	odd	even	odd	odd	even

$i, k = 0, 1, 2, \dots, \infty$ , are the number of the harmonic functions in the  $X_1$  and  $X_3$  directions, respectively. The harmonics  $\Psi_{ik}^m, \varphi_{ik}^m$ , and  $\phi_{ik}^m$  are given as follows:

$$\begin{aligned} \Psi_{ik}^1 &= \cos \frac{i\pi X_1}{r_1} \sin \frac{k\pi X_3}{r_3}, & \varphi_{ik}^1 &= \sin \frac{i\pi X_1}{r_1} \cos \frac{k\pi X_3}{r_3}, & \phi_{ik}^1 &= \cos \frac{i\pi X_1}{r_1} \sin \frac{k\pi X_3}{r_3}, \\ \Psi_{ik}^2 &= \sin \frac{i\pi X_1}{r_1} \cos \frac{k\pi X_3}{r_3}, & \varphi_{ik}^2 &= \cos \frac{i\pi X_1}{r_1} \sin \frac{k\pi X_3}{r_3}, & \phi_{ik}^2 &= \sin \frac{i\pi X_1}{r_1} \sin \frac{k\pi X_3}{r_3}, \\ \Psi_{ik}^3 &= \cos \frac{i\pi X_1}{r_1} \cos \frac{k\pi X_3}{r_3}, & \varphi_{ik}^3 &= \sin \frac{i\pi X_1}{r_1} \sin \frac{k\pi X_3}{r_3}, & \phi_{ik}^3 &= \cos \frac{i\pi X_1}{r_1} \sin \frac{k\pi X_3}{r_3}, \\ \Psi_{ik}^4 &= \sin \frac{i\pi X_1}{r_1} \sin \frac{k\pi X_3}{r_3}, & \varphi_{ik}^4 &= \cos \frac{i\pi X_1}{r_1} \cos \frac{k\pi X_3}{r_3}, & \phi_{ik}^4 &= \sin \frac{i\pi X_1}{r_1} \cos \frac{k\pi X_3}{r_3}. \end{aligned} \tag{14}$$

Substitution of (13) into (12), after some manipulations, results in the following algebraic system:

$$\mathbf{M}^m \mathbf{a} = 0, \quad m = 1, 2, 3, 4, \tag{15}$$

where  $\mathbf{M}^m$  and  $\mathbf{a}$  are the coefficient matrices containing the unknown strain parameters  $b$  and  $d$  and the amplitude vector,  $\mathbf{a} = (A_{ik}, B_{ik}, V_{ik}^n)^T$ , respectively. A nontrivial solution  $\mathbf{a}$  of (15) exists when

$$|\mathbf{M}^m| = 0, \quad m = 1, 2, 3, 4. \tag{16}$$

The critical value of the compressive strain  $b$  for prescribed  $d$  (or of  $d$  for prescribed  $b$ ) can be obtained as the smallest positive root of (16).

Turning attention to (12) we identify the leading approximating system as the two equations  $C_0 = 0$  and  $D_0 = 0$  with only the functions  $A_0$  and  $B_0$  being present and all  $V_n = 0$ . This system is:

$$C_0 \equiv \beta_{11}(X_3)A_{0,11} + \beta_{12}(X_1)A_{0,33} + b_{13}B_{0,13} = 0, \tag{17a}$$

$$D_0 \equiv \beta_{31}(X_3)B_{0,11} + \beta_{32}(X_1)B_{0,33} + b_{13}A_{0,13} = 0, \tag{17b}$$

which reduces to the two-dimensional system considered in Lagoudas *et al.* (1991) by setting either  $r'_2 = r_2$  and  $b = 0$  or  $r'_2 = 0$  and  $d = 0$ .

The simplest possible approximation to a solution of (17), for each case, is obtained when the terms with either  $i = 0$  and  $k = 1$  or  $i = 1$  and  $k = 0$  are nonzero and all other  $A_{ik}$  and  $B_{ik}$  are set to zero. In that case the following possible solutions are obtained:

Case 1

Either

$$\left\{ (1-2b)G_{13} - bE_{13} - d[E_{33}^h(1-r'_2/r_2) + \frac{1}{2}C_0^*r'_2/r_2] \right\} \left( \frac{\pi}{r_3} \right)^2 A_{01} = 0 \tag{18a}$$

or

$$\left\{ (1-2d)G_{13} - dE_{13} - b[E_{11}^v(r'_2/r_2) + \frac{1}{2}D_0^*(1-r'_2/r_2)] \right\} \left( \frac{\pi}{r_1} \right)^2 B_{10} = 0. \tag{18b}$$

Case 2

Either

$$\left\{ (1-3b)[E_{11}^v(r'_2/r_2) + \frac{1}{2}D_0^*(1-r'_2/r_2)] - dE_{13} \right\} \left( \frac{\pi}{r_1} \right)^2 A_{10} = 0 \tag{19a}$$

or

$$\{(1-3d)[E_{33}^h(1-r'_2/r_2) + \frac{1}{2}C_0^*(r'_2/r_2)] - bE_{13}\} \left(\frac{\pi}{r_3}\right)^2 B_{01} = 0. \quad (19b)$$

Case 3

Either

$$\{(1-2b)G_{13} - bE_{13} - d[E_{33}^h(1-r'_2/r_2) + \frac{1}{2}C_0^*(r'_2/r_2)]\} \left(\frac{\pi}{r_3}\right)^2 A_{01} = 0 \quad (20a)$$

or

$$\{(1-3b)[E_{11}^v(r'_2/r_2) + \frac{1}{2}D_0^*(1-r'_2/r_2)] - dE_{13}\} \left(\frac{\pi}{r_1}\right)^2 A_{10} = 0. \quad (20b)$$

Case 4

Either

$$\{(1-3d)[E_{33}^h(1-r'_2/r_2) + \frac{1}{2}C_0^*(r'_2/r_2)] - bE_{13}\} \left(\frac{\pi}{r_3}\right)^2 B_{01} = 0 \quad (21a)$$

or

$$\{(1-2d)G_{13} - dE_{13} - b[E_{11}^v(r'_2/r_2) + \frac{1}{2}D_0^*(1-r'_2/r_2)]\} \left(\frac{\pi}{r_1}\right)^2 B_{10} = 0. \quad (21b)$$

It is noted that in the absence of the plies with horizontal fibers ( $r'_2 = r_2$ ) and without compression in the  $X_1$  direction ( $b = 0$ ) eqns (18a) and (20a) coincide with Rosen's classical result (1956) for compressive buckling strain of fibrous composites in the shear buckling mode. That is, they reduce to

$$d = \frac{2G_{13}}{C_0^*} \approx \frac{G_m}{E_f C_f (1 - C_f)}, \quad (22)$$

where the subscripts f and m denote the fiber and the matrix, respectively. Similarly, without the plies with vertical fibers ( $r'_2 = 0$ ) of the composite, the same buckling strain of shear mode of fibrous composites as derived from Rosen's analysis (1956) can be obtained from (18b) and (21b) when compression is applied in the  $X_1$  direction only ( $d = 0$ ). As mentioned previously, the vanishing of the coefficient functions  $C_j$  and  $D_j$ ,  $j = 0, 1, 2, \dots$ , in (12) provides two infinite sets of equations in the  $X_2$  direction. Therefore, not only are the larger values of  $i$  and  $k$  of (14) taken into account (more nonzero terms in  $X_1$  and  $X_3$  directions) but a higher value of  $j$  is used in (12) (more sets of equations). It should be noted that the potential functions  $V_n$  are not present in the leading approximating system [ $j = 0$ ; eqn (17)] but they appear in the system for  $j \geq 1$ . Therefore, the approximating system for  $j = 1$  consists of the four equations  $C_0 = 0$ ,  $D_0 = 0$ ,  $C_1 = 0$  and  $D_1 = 0$  with  $A_0$ ,  $B_0$  and  $V_1$  being present, and is given by:

$$C_0 = \beta_{11}(X_3)A_{0,11} + \beta_{12}(X_1)A_{0,33} + b_{13}B_{0,13} \\ + \frac{1}{2}K_3\beta_{13}(X_3)\alpha_1^{(2)}V_{1,311} + \frac{1}{2}K_3\beta_{14}(X_1)\alpha_1^{(2)}V_{1,333} = 0, \quad (23a)$$

$$D_0 = \beta_{31}(X_3)B_{0,11} + \beta_{32}(X_1)B_{0,33} + b_{13}A_{0,13} \\ - \frac{1}{2}K_1\beta_{33}(X_3)\alpha_1^{(2)}V_{1,111} - \frac{1}{2}K_1\beta_{34}(X_1)\alpha_1^{(2)}V_{1,133} = 0, \quad (23b)$$

$$C_1 = \beta_{13}(X_3)\alpha_1^{(2)}A_{0,11} + \beta_{14}(X_1)\alpha_1^{(2)}A_{0,33} + (K_3\beta_{11}(X_3) \\ - K_1b_{13})V_{1,311} + \frac{1}{2}K_3\beta_{13}(X_3)\alpha_2^{(2)}V_{1,311} + K_3\beta_{12}(X_1)V_{1,333} \\ + \frac{1}{2}K_3\beta_{14}(X_1)\alpha_1^{(2)}V_{1,333} - K_3b_{12}\left(\frac{\pi}{r_2}\right)^2 V_{1,3} = 0, \quad (23c)$$



$$\begin{aligned}
 D_1 = & \beta_{33}(X_3)\alpha_1^{(2)}B_{0,33} + \beta_{34}(X_1)\alpha_1^{(2)}B_{0,33} - (K_1\beta_{32}(X_1) \\
 & - K_3b_{13})V_{1,133} - \frac{1}{2}K_1\beta_{33}(X_3)\alpha_2^{(2)}V_{1,111} - K_1\beta_{31}(X_3)V_{1,111} \\
 & - \frac{1}{2}K_1\beta_{34}(X_1)\alpha_2^{(2)}V_{1,133} + K_1b_{32}\left(\frac{\pi}{r_2}\right)^2V_{1,1} = 0. \quad (23d)
 \end{aligned}$$

It is mentioned here that the results reported in this paper are based on the system given by (23). The values of  $i$  and  $k$  in the harmonic functions  $\Psi_{ik}^m$ ,  $\varphi_{ik}^m$  and  $\phi_{ik}^m$ , with  $m = 1, 2, 3, 4$  of the functions  $A_0$ ,  $B_0$  and  $V_1$ , respectively, are taken into account up to and including 1. Also, since the lowest modal number for sine function is 1, then (23) becomes a  $8 \times 8$ ,  $6 \times 6$ ,  $7 \times 7$ , and  $7 \times 7$  algebraic system for cases 1–4 respectively. The convergence of the solutions is tested by comparison with higher order systems  $j \geq 2$ . Only negligible differences were observed and it was decided to stop the calculations with  $j = 1$ .

It is noted that when the plies with horizontal fibers are absent ( $r'_2 = r_2$ ) the terms

$$\alpha_n^{(2)}, \alpha_n^{(i)} = \frac{2}{n\pi} \sin\left(\frac{n\pi r_i}{r_i}\right), \quad i = 1, 2, 3,$$

in (12) are zero which means that the functions  $A_0$  and  $B_0$  are not present in equations  $C_j$  and  $D_j$  for  $j \geq 1$ . Thus, eqns (12a<sub>1</sub>) and (12b<sub>1</sub>) in the 2-D case become independent of  $V_n$ . This system therefore represents the behavior of the 2-D case and all terms involving  $V_n$  disappear in this case.

NUMERICAL RESULTS AND DISCUSSIONS

As mentioned before, the critical strain of the one term approximation with different modes of buckling is given by (18)–(21). Under certain conditions, as mentioned previously, some of those equations reduce to Rosen’s classical results (1956) for compressive buckling strain of fibrous composites in the shear buckling mode.

For higher order approximation, (16) is solved numerically with given values of  $h$  representing compression in the  $X_1$  direction to obtain critical compressive strength of the composite in the  $X_3$  direction.

To study the special 2-D case ( $r'_2 = r_2$ ) with uniaxial compression in the  $X_3$  direction ( $h = 0$ ), we note that in the absence of cross plies the spacing parameter  $r_3$  becomes a free parameter and can be interpreted as a measure of wavelength of imperfections (Lagoudas *et al.*, 1991). In that case, the effect of imperfections, normalized as the ratio  $r_3/r_1$ , on the critical compressive strain  $d$  for various modes of buckling given by the symmetry cases 1–4 is shown in Fig. 2. In this figure,  $C_f^i$  is set to be 0.5 and the properties of glass ( $E_f = 72.3$  Gpa,  $\nu_f = 0.22$ ) with two choices of epoxy,  $G_m = 1.306$  Gpa,  $\nu_m = 0.302$  (solid lines) and  $G_m = 1.0815$  Gpa,  $\nu_m = 0.35$  (dashed lines) are selected. This figure clearly shows that in the two-dimensional case the critical strains obtained from cases 1 and 2 coincide with cases 3 and 4 respectively showing that only shear and extensional modes of buckling are present. It is also observed that the resistance to fiber buckling of the composites can be improved by increasing the shear modulus of the matrix. As reported in Lagoudas *et al.* (1991), the minimum value of critical strain  $d$  occurs in the limit of minute imperfections, i.e.  $r_3/r_1$  tends to zero. The detailed discussion about the 2-D case can be found in Lagoudas *et al.* (1991).

Considering the 3-D case, the properties of glass/epoxy system ( $E_f = 72.3$  Gpa,  $\nu_f = 0.22$ ,  $E_m = 2.92$  Gpa and  $\nu_m = 0.35$ ) is used. It is noted from the definition of the normalized spacing ratios  $r_3/r_1$  and  $r_3/r_2$  in (23) that we can write  $r_3/r_1 = (C_f^i/C_f^h)(r'_3/r'_1)$  and  $r_3/r_2 = (r'_1/r'_2)(r_3/r_1/C_f^i)(r'_2/r_2)$ , where  $0 \leq (C_f^i, C_f^h) \leq 1$ . This allows us to vary certain

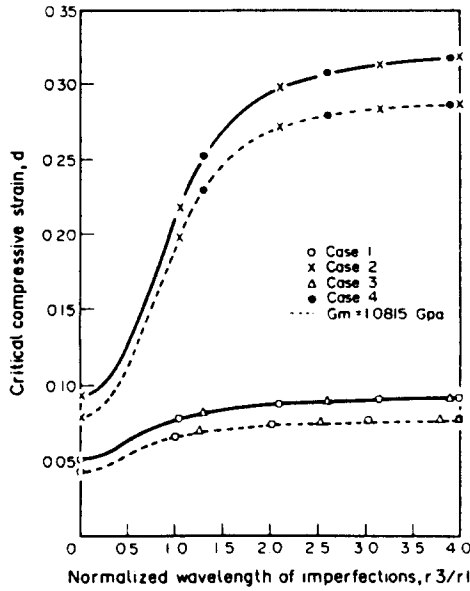


Fig. 2. The effect of normalized wavelength of imperfections  $r_3/r_1$  on critical compressive strain  $d$  for  $r'_2 = r_2$ ,  $b = 0$  and  $C_1^* = 0.5$ .

physical parameters while keeping the remaining parameters fixed and thus determine the effect of variation of these parameters upon the critical compressive strain.

To study the occurrence of the modes with various symmetries during buckling the critical strain  $d$  is plotted against the critical strain  $b$  in Fig. 3. In this figure, the values of parameters used are  $C_1^* = C_1^b = 0.5$ ,  $r'_1 = r'_3$ ,  $r'_2 = 10r'_1$  and  $r'_2 = 0.5r_2$  and therefore  $r_3/r_2 = 0.1$ . It is observed that at the beginning,  $d$  is a monotonic decreasing function of  $b$ . Also, as  $b$  increases from zero the buckling occurs either by the symmetry case 1 or 3 and these coincide for a limited interval of  $b$ . Thereafter, cases 1 and 4 coincide and determine the critical condition.

To investigate the effect of ply layup on the solutions, critical strain  $d$  versus  $\mu$ , in which  $\mu \equiv (r_2 - r'_2)/r_2$ , for various values of  $b$  are plotted in Figs 4-6. In those figures  $C_1^* = C_1^b = 0.5$ ,  $r'_1 = r'_3$ , and  $r_3/r_1 = 1.0$ . The strains given in the horizontal direction in

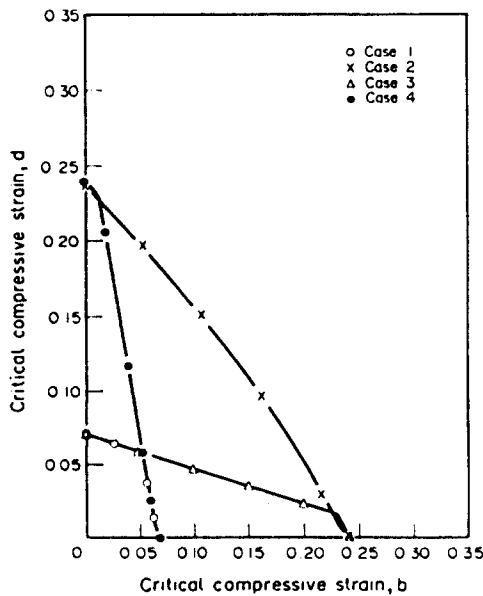


Fig. 3. Critical strain  $d$  vs critical strain  $b$  with the parameters  $r'_2 = 0.5r_2$ ,  $C_1^b = C_1^* = 0.5$ ,  $r'_1 = r'_3$  and  $r'_2 = 10r'_1$ .

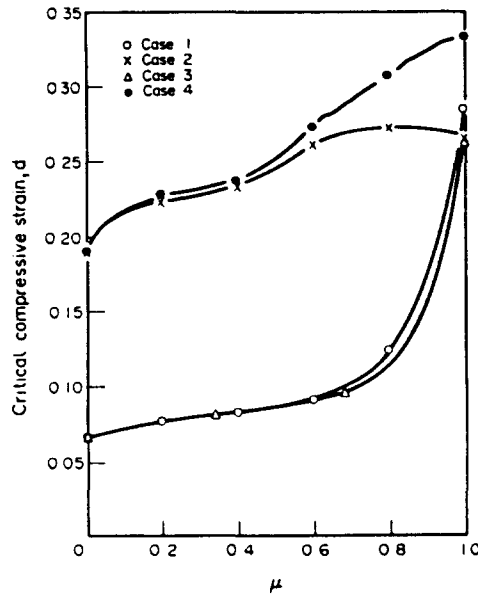


Fig. 4. Buckling strain  $d$  vs  $\mu$  for  $b = 0$ ,  $C_1^h = C_1^v = 0.5$ ,  $r_1^v = r_1^h$  and  $r_1 = r_2$ .

these figures are, respectively,  $b = 0, 0.04$  and  $0.07$ . It should be noted that perfect bond between each layer is assumed. Also,  $\mu$  denotes the normalized thickness of the lamina with horizontal fibers that is present in one period in the  $X_2$  direction. It is seen from Fig. 4 that under uniaxial loading condition ( $b = 0$ ) the buckling strain determined by either case 1 or 3, increases with  $\mu$ . That is, additional resistance to fiber buckling is provided by adjacent plies as the thicknesses of these plies increase in the  $X_2$  direction. This phenomenon was also found by Swanson (1990). However, as shown in Figs 5 and 6, when the strain  $b$  is nonzero, the buckling strain  $d$  increases within an interval of  $\mu$  and thereafter decreases with  $\mu$ . This observation is opposite to the result obtained by uniaxial compression as shown in Fig. 4.

The effect of fiber volume fraction of the laminas with horizontal fibers on the critical strain of the structure in the vertical direction is shown in Fig. 7. In this figure critical strain  $d$  is plotted as a function of  $C_1^h$  with a fixed value of  $b$ . The parameters used in this figure

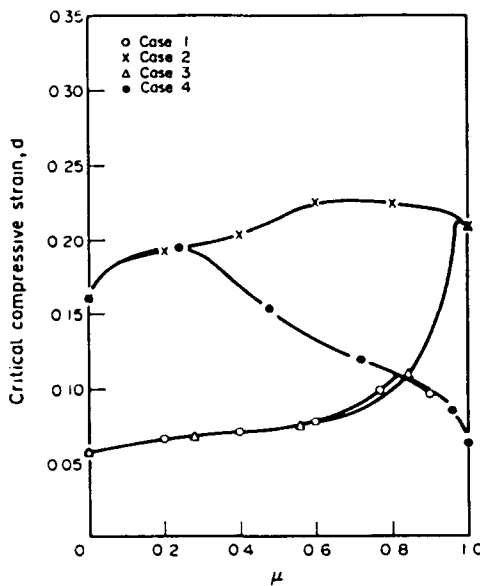


Fig. 5. Buckling strain  $d$  vs  $\mu$  for  $b = 0.04$ ,  $C_1^h = C_1^v = 0.5$ ,  $r_1^v = r_1^h$  and  $r_1 = r_2$ .

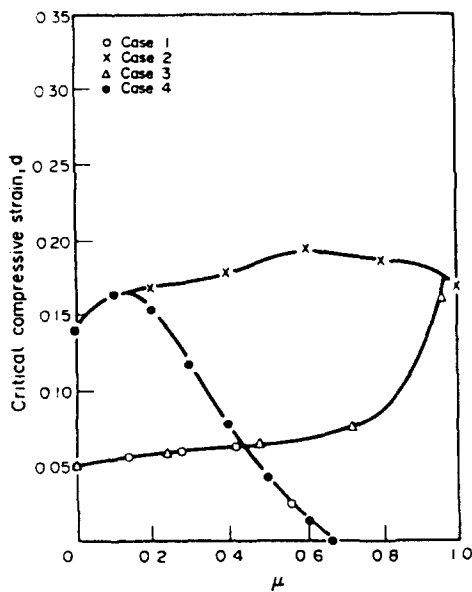


Fig. 6. Buckling strain  $d$  vs  $\mu$  for  $b = 0.07$ ,  $C_1^* = C_1^h = 0.5$ ,  $r_1' = r_1$  and  $r_3 = r_1$ .

are  $b = 0$ ,  $C_1^* = 0.5$ ,  $r_2' = 0.5r_2$ ,  $r_2' = 10r_1$  and  $r_3 = r_1$ . The result shows that the critical compressive strain  $d$  monotonically increases with  $C_1^h$  and that buckling is governed by either case 1 or 3 both of which predict almost the same value.

CONCLUSION

The Fourier-series-based analytical approach appears to be capable of analysing the occurrence of microbuckling in cross-ply composite laminates. The difficulty of solving separate problems in fiber and matrix phases and matching conditions across the interfaces is overcome. However, this has been achieved at the expense of assuming a rectangular periodic arrangement of matrix and fibers at the microstructural level. Computationally the method is efficient and conveys rapidly. The numerical results have the expected behavior

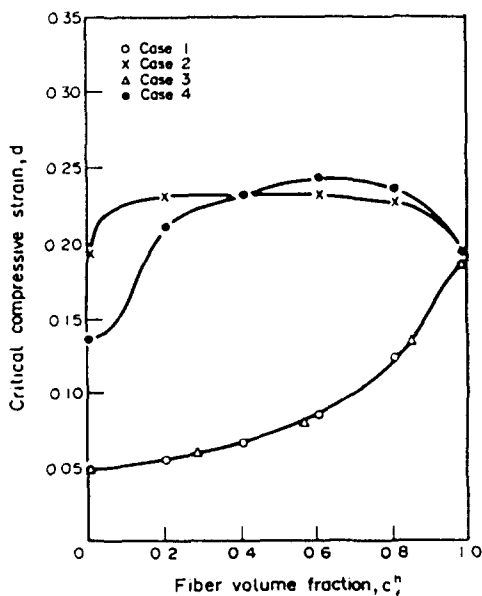


Fig. 7. Critical strain  $d$  vs  $C_1^h$  for  $b = 0$ ,  $C_1^* = 0.5$ ,  $r_2' = 10r_1$ ,  $r_2' = 0.5r_2$  and  $r_3 = r_1$ .

and as shown in prior investigation (Lagoudas *et al.*, 1991), agree substantially with experimental results.

REFERENCES

Chung, W. Y. and Testa, R. B. (1969). The elastic stability of fibers in a composite plate. *J. Comp. Mater.* 3, 58-80.  
 Lagoudas, D. C., Tadjbakhsh, I. G. and Fares, N. (1991). A new approach to microbuckling of fibrous composites. *J. Appl. Mech.* 58, 473-479.  
 Malvern, L. E. (1969). *Introduction to the Mechanics of a Continuous Medium*. Prentice-Hall, NJ.  
 Rosen, B. W. (1956). *Mechanics of Composite Strengthening, in Fiber Composite Materials*. American Society for Metals, Metals Park, OH.  
 Stief, P. S. (1988). A simple model for the compressive failure of weakly bonded, fiber-reinforced composites. *J. Comp. Mater.* 22, 818-828.  
 Swanson, S. R. (1990). A micro-mechanics model for compression failure of fiber composite laminates. *27th Annual Technical Meeting of Society of Engineering Science*, Santa Fe.

APPENDIX A

Hooke's law is expressed as

$$\sigma = L\varepsilon,$$

where

$$\sigma = (\sigma_{11}, \sigma_{22}, \sigma_{11}, \sigma_{23}, \sigma_{11}, \sigma_{12})^T,$$

$$\varepsilon = (\varepsilon_{11}, \varepsilon_{22}, \varepsilon_{11}, 2\varepsilon_{23}, 2\varepsilon_{13}, 2\varepsilon_{12})^T,$$

and

$$\varepsilon_{ij} = \frac{1}{2} \left( \frac{\partial u_i}{\partial X_j} + \frac{\partial u_j}{\partial X_i} + \frac{\partial u_k}{\partial X_i} \frac{\partial u_k}{\partial X_j} \right), \quad i, j, k = 1, 2, 3.$$

Here  $u_i$  are the components of the displacement vector  $u$  defined by  $u_i = x_i - X_i$ . Also

$$L = S^{-1} = \begin{bmatrix} \frac{1}{E_1} - \frac{\nu_{12}}{E_1} - \frac{\nu_{13}}{E_1} & 0 & 0 & 0 \\ \frac{1}{E_2} - \frac{\nu_{23}}{E_2} & 0 & 0 & 0 \\ \frac{1}{E_3} & 0 & 0 & 0 \\ \text{symm.} & \frac{1}{G_{23}} & 0 & 0 \\ & & \frac{1}{G_{13}} & 0 \\ & & & \frac{1}{G_{12}} \end{bmatrix}^{-1}$$

$$\equiv \begin{bmatrix} E_{11} & E_{12} & E_{13} & 0 & 0 & 0 \\ & E_{22} & E_{23} & 0 & 0 & 0 \\ & & E_{33} & 0 & 0 & 0 \\ \text{symm.} & & & G_{23} & 0 & 0 \\ & & & & G_{13} & 0 \\ & & & & & G_{12} \end{bmatrix}.$$

where  $S$  is the compliance matrix for an orthotropic elastic medium.

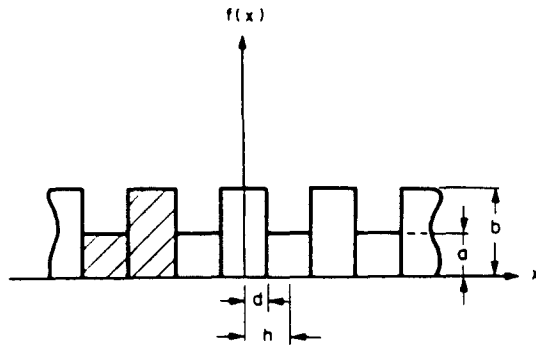


Fig. A1. Fourier series representation.

APPENDIX B

Defining  $f(x)$  as an even periodic function (see Fig. A1) it can be expressed as a series of cosine terms:

$$f(x) = \frac{1}{2}f_0 + \sum_{n=1}^{\infty} f_n \cos \frac{n\pi X}{h} \tag{B1}$$

where

$$f_0 = 2[bd + (h-d)a] = 2bd + (2h-2d)a = \text{shaded area}, \tag{B2}$$

$$f_n = \frac{2}{h} \int_0^h f(x) \cos \frac{n\pi X}{h} dx = \frac{2(b-a)}{n\pi} \sin \frac{n\pi d}{h}, \quad n = 1, 2, 3, \dots \tag{B3}$$

Referring to Fig. 1(a), let  $E_{11}^v$  be the axial Young's modulus for the laminae with vertical fibers, which is a periodic function in the  $X_1$  direction, so that we have from (B1) (B3):

$$E_{11}^v(X_1) = \left[ E_i \left( \frac{r'_1}{r_1} \right) + E_m \left( 1 - \frac{r'_1}{r_1} \right) \right] + (E_i - E_m) \sum_{n=1}^{\infty} x_n^{(1)} \cos \frac{n\pi X_1}{r_1} \tag{B4}$$

Similarly, let  $E_{11}^h$  be the axial Young's modulus for the layers with horizontal fibers then

$$E_{11}^h(X_1) = \left[ E_i \left( \frac{r'_1}{r_1} \right) + E_m (1 - r'_1/r_1) \right] + (E_i - E_m) \sum_{n=1}^{\infty} x_n^{(1)} \cos \frac{n\pi X_1}{r_1} \tag{B5}$$

We now consider the composite which is also periodic in the  $X_2$  direction:

$$E_{11}(X_2, X_1) = E_{11}^v(r'_2/r_2) + E_{11}^h(X_1)(1 - r'_2/r_2) + [E_{11}^v - E_{11}^h(X_1)] \sum_{n=1}^{\infty} x_n^{(2)} \cos \frac{n\pi X_2}{r_2} \tag{B6}$$

$$E_{33}(X_1, X_2) = E_{33}^v(r'_2/r_2) + E_{33}^h(X_1)(1 - r'_2/r_2) + [E_{33}^v(X_1) - E_{33}^h] \sum_{n=1}^{\infty} x_n^{(2)} \cos \frac{n\pi X_2}{r_2} \tag{B7}$$

where

$$x_n^{(i)} = \frac{2}{2\pi} \sin \frac{n\pi r'_i}{r_i}, \quad i = 1, 2, 3.$$

APPENDIX C

The differential operator in eqn (7) has the following components

$$\mathcal{L} = \begin{bmatrix} \mathcal{L}_{11} & \mathcal{L}_{12} & \mathcal{L}_{13} \\ \mathcal{L}_{12} & \mathcal{L}_{22} & \mathcal{L}_{23} \\ \mathcal{L}_{13} & \mathcal{L}_{23} & \mathcal{L}_{33} \end{bmatrix}$$

$$\begin{aligned} \mathcal{L}_{11} &= [(1-3b)E_{11} - dE_{13}] \frac{\partial^2}{\partial X_1^2} + [(1-2b)G_{12} - (bE_{12} + dE_{23})] \frac{\partial^2}{\partial X_2^2} + [(1-2b)G_{13} - (bE_{13} + dE_{33})] \frac{\partial^2}{\partial X_3^2}, \\ \mathcal{L}_{12} &= (1-2b)^{1/2} (G_{12} + E_{12}) \frac{\partial^2}{\partial X_1 \partial X_2}, \\ \mathcal{L}_{13} &= (1-2b)^{1/2} (1-2d)^{1/2} (G_{13} + E_{13}) \frac{\partial^2}{\partial X_1 \partial X_3}, \\ \mathcal{L}_{22} &= (-bE_{11} + G_{12} - dE_{13}) \frac{\partial^2}{\partial X_1^2} + (E_{22} - bE_{12} - dE_{23}) \frac{\partial^2}{\partial X_2^2} + (G_{23} - dE_{33} - bE_{13}) \frac{\partial^2}{\partial X_3^2}, \\ \mathcal{L}_{23} &= (1-2d)^{1/2} (G_{23} + E_{23}) \frac{\partial^2}{\partial X_2 \partial X_3}, \\ \mathcal{L}_{33} &= [(1-2d)G_{13} - (bE_{11} + dE_{13})] \frac{\partial^2}{\partial X_1^2} + [(1-2d)G_{23} - (bE_{12} + dE_{23})] \frac{\partial^2}{\partial X_2^2} + [(1-3d)E_{33} - bE_{13}] \frac{\partial^2}{\partial X_3^2}. \end{aligned}$$

APPENDIX D

$$\begin{aligned} \beta_{11}(X_1) &= [(1-3b)E_{11}^0 - dE_{13}] + (1-3b)(1-r'_2/r_2) \sum_{n=1}^{\infty} D_n^* \cos \frac{n\pi X_1}{r_1} \equiv \sum_{n=0}^{\infty} \beta_{11}^n \cos \frac{n\pi X_1}{r_1}, \\ \beta_{12}(X_1) &= [(1-2b)G_{12} - bE_{12} - dE_{23}] + d(r'_2/r_2) \sum_{n=1}^{\infty} C_n^* \cos \frac{n\pi X_1}{r_1} \equiv \sum_{n=0}^{\infty} \beta_{12}^n \cos \frac{n\pi X_1}{r_1}, \\ \beta_{13}(X_1) &= \left[ (1-3b)(E_{11}^0 - \frac{1}{2}D_0^*) - \sum_{n=1}^{\infty} D_n^* \cos \frac{n\pi X_1}{r_1} \right] \equiv \sum_{n=0}^{\infty} \beta_{13}^n \cos \frac{n\pi X_1}{r_1}, \\ \beta_{14}(X_1) &= -d \left[ (\frac{1}{2}C_0^* - E_{13}^0) + \sum_{n=1}^{\infty} C_n^* \cos \frac{n\pi X_1}{r_1} \right] \equiv \sum_{n=0}^{\infty} \beta_{14}^n \cos \frac{n\pi X_1}{r_1}, \\ \beta_{11}(X_1) &= [(1-2d)G_{13} - dE_{13} - bE_{13}^0] - b(1-r'_2/r_2) \sum_{n=1}^{\infty} D_n^* \cos \frac{n\pi X_1}{r_1} \equiv \sum_{n=0}^{\infty} \beta_{11}^n \cos \frac{n\pi X_1}{r_1}, \\ \beta_{12}(X_1) &= [(1-3d)E_{11}^0 - bE_{11}^0] + (1-3d)(r'_2/r_2) \sum_{n=1}^{\infty} C_n^* \cos \frac{n\pi X_1}{r_1} \equiv \sum_{n=0}^{\infty} \beta_{12}^n \cos \frac{n\pi X_1}{r_1}, \\ \beta_{13}(X_1) &= -b \left[ (E_{11}^0 - \frac{1}{2}D_0^*) - \sum_{n=1}^{\infty} D_n^* \cos \frac{n\pi X_1}{r_1} \right] \equiv \sum_{n=0}^{\infty} \beta_{13}^n \cos \frac{n\pi X_1}{r_1}, \\ \beta_{14}(X_1) &= (1-3d) \left[ (\frac{1}{2}C_0^* - E_{13}^0) + \sum_{n=1}^{\infty} C_n^* \cos \frac{n\pi X_1}{r_1} \right] \equiv \sum_{n=0}^{\infty} \beta_{14}^n \cos \frac{n\pi X_1}{r_1}, \\ E_{11}^0 &= E_{11}^0 r'_2/r_2 + \frac{1}{2}D_0^*(1-r'_2/r_2), \\ E_{13}^0 &= E_{13}^0(1-r'_2/r_2) + \frac{1}{2}C_0^*(r'_2/r_2), \\ b_{11} &= (1-2b)^{1/2} (1-2d)^{1/2} (G_{13} + E_{13}), \\ b_{12} &= [(1-2b)G_{12} - (bE_{12} + dE_{23})], \\ b_{13} &= [(1-2d)G_{23} - (bE_{12} + dE_{23})]. \end{aligned}$$